ELSEVIER

Chemical Engineering Journal 71 (1998) 23–35

Chemical Engineering Journal

Mixed specification problems in large-scale pipeline networks

Chee Seng Lim, Hwei Chen Ti*

Department of Chemical Engineering, National University of Singapore, 10 Kent Ridge Crescent, Singapore 119260, Singapore

Received 22 September 1997; received in revised form 22 May 1998; accepted 3 June 1998

Abstract

The solution of pipe network problems can usually be obtained by orthogonal mesh and nodal approaches. However, when the size of a network becomes very large, these methods may not be efficient. In such a case diakoptics may be used. Essentially this approach tears the given network into two or more smaller subnetworks, thereby reducing the size of the matrices involved and saving computation time. So far most research in the area of diakoptics has been confined to problems where all the external flows are specified. Although the fictitious branch method has been incorporated into diakoptics to solve mixed flow- and pressure-specified problems it cannot satisfactorily solve problems with many pressure specified nodes. In the present work, a method for solving mixed specification problems is developed based on mesh and nodal diakoptics, incorporating partitioning. The diakoptics technique for the solution of mixed specification problems is found to be more efficient than conventional partitioning methods.

Keywords: Pipeline network; Mesh and nodal approaches; Diakoptics; Partitioning; Transformation; Mixed specification

1. Introduction

Various research [2–5] has shown that most pipe network problems can be solved by orthogonal mesh and nodal approaches. However, these approaches have been confined to problems where all external flows are specified. For mixed specification problems, two methods were developed, namely, the fictitious branch method and the partitioning method. These methods are satisfactory in so far as the size of the network is not too large. For extremely large-scale networks, the mesh and nodal methods may not be efficient due to an increase in computation time. To counter this problem the technique of diakoptics can be applied [1,6–8]. This approach tears the given network into a number of smaller subnetworks, which can then be solved more efficiently. Although the fictitious branch method has been extended to the diakoptics methods, it cannot efficiently solve problems with many pressure specified nodes. This is because the introduction of one or two fictitious branches to each pressure specified node increases the size of the network. The partitioning method on the other hand will not increase the size of the network but it has not been extended to the diakoptics methods.

*Corresponding author. Tel.: +65-8742188; fax: +65-7791936; e-mail: chetihc@nus.edu

2. Transformation theory

In the diakoptics approach there are three major reference frames pertaining to a network: the primitive framework, the orthogonal framework and the torn framework. The primitive framework treats each branch of a network as disconnected, individual units. It is in this framework that the Eq. (1) expressing the relationship between pressure drop and flow, known as the governing equation, applies.

$$\Delta P = \frac{32\rho\phi_f L Q^2}{\pi^2 D^5} \tag{1}$$

The orthogonal framework represents the network with its interconnections. In this reference frame open and closed paths exist for flows and pressure drops. Open path flows are represented by flows from external sources and are constrained in node-to-datum paths, while closed path flows carry the response due to other sources and are constrained in meshes. The orthogonal reference frame is the one in which the solution of pipe network problems is most meaningful. The torn framework shows the network configuration after it is dissected into several sub-units. It is in this reference frame that diakoptics may be applied. The relationship between the different reference frames is described by transformation tensors.

A tensor is a matrix that carries in its notation a superscript index, a subscript index, or both, for the purpose of

1385-8947/98/$ – see front matter
PII: S1385-8947(98)00109-0

indicating the reference frame under which variables such as flow are considered, and for indicating the direction of the transformation (i.e. from primitive to orthogonal, or orthogonal to torn) in the case of transformation tensors. The following indices are used for the various frameworks: b for primitive, s for orthogonal, o for open path, c for closed path, and p for torn framework. Flow and pressure are distinguished by a superscript and subscript notation, respectively. For example, the flow vector in the primitive framework is represented by the tensor $\boldsymbol{J}^{\mathrm{b}}$ (contravariant tensor) while the pressure vector is represented by $\boldsymbol{V}_{\mathrm{b}}$ (covariant tensor) [4].

3. Diakoptics

In the diakoptics approach the given network is cut and torn into several subnetworks, which together constitute an intermediate reference frame known as the torn framework. The method of tearing varies according to whether mesh diakoptics or nodal diakoptics is applied.

Although in principle there is no restriction on the number of subnetworks into which a given network may be torn, the following derivation of the mesh and nodal diakoptics method for solving mixed specification problems is based on tearing the given network into three subnetworks: subnetworks 1 and 2, and a removed subnetwork.

3.1. Mesh partitioning diakoptics

This method is so called because the matrices to be inverted are of the same size (order) of the meshes of the subnetworks, and its derivation begins with a form that is similar to the fundamental equation employed for the mesh partitioning approach [5]. Furthermore, in the solution of fully flow-specified problems using this approach, the mesh currents are first calculated, from which the nodal pressures are then determined.

In mesh diakoptics the tearing is always such that the removed subnetwork is made up of tree branches and their nodes, that is, no closed loops are allowed. For example, consider the network SIMP in Fig. 1. This network can be cut as in Fig. 2, and the torn configuration represented in Fig. 3. Note that after the network is torn the links which were originally connected to the nodes associated with the removed subnetwork are now connected directly to the datum node.

The relationships between flow in the orthogonal and torn frameworks are:

$$\boldsymbol{J}^{\mathrm{s}} = \boldsymbol{C}^{\mathrm{s}}_{\cdot\mathrm{p}}\boldsymbol{J}^{\mathrm{p}} \tag{2}$$

$$\boldsymbol{J}^{\mathrm{p}} = \boldsymbol{A}^{\mathrm{p}}_{\cdot\mathrm{s}}\boldsymbol{J}^{\mathrm{s}} \tag{3}$$

The relationships between pressure in the orthogonal and torn frameworks are:

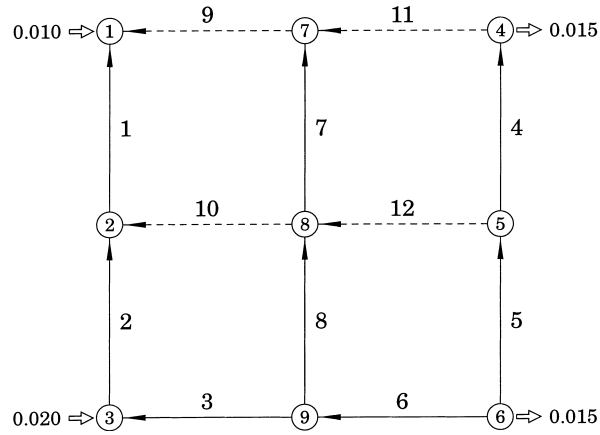

Fig. 1. Network SIMP.

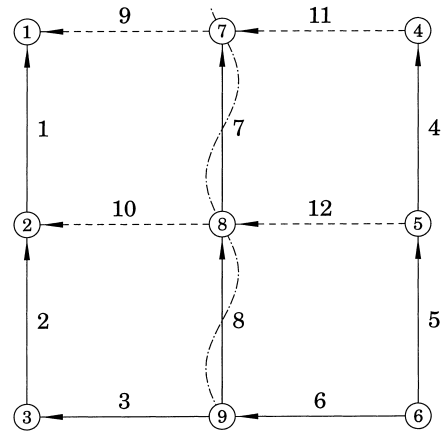

Fig. 2. Network SIMP cut by mesh diakoptics.

$$\boldsymbol{V}_{\mathrm{s}} = \boldsymbol{A}^{\cdot\mathrm{p}}_{\mathrm{s}}\boldsymbol{V}_{\mathrm{p}} \tag{4}$$

$$\boldsymbol{V}_{\mathrm{p}} = \boldsymbol{C}^{\cdot\mathrm{s}}_{\mathrm{p}}\boldsymbol{V}_{\mathrm{s}} \tag{5}$$

The various relevant tensors are first partitioned into subnetworks 1, 2 and the removed subnetwork, and then further partitioned into flow-specified and pressure specified components. Flow-specified components are indicated by the letter f while pressure-specified components by the letter p, appearing as the last letter in the subscript of components A_{T}, A_{L} and B_{T}.

$$\boldsymbol{A}^{\cdot\mathrm{s}}_{\mathrm{b}} = \begin{bmatrix} A_{\mathrm{T1f}} & A_{\mathrm{T1p}} & 0 & 0 & 0 & 0 & 0 & 0 \\ 0 & 0 & A_{\mathrm{T2f}} & A_{\mathrm{T2p}} & 0 & 0 & 0 & 0 \\ 0 & 0 & 0 & 0 & A_{\mathrm{TRf}} & A_{\mathrm{TRp}} & 0 & 0 \\ A_{\mathrm{L1f}} & A_{\mathrm{L1p}} & 0 & 0 & A_{\mathrm{L3f}} & A_{\mathrm{L3p}} & U_{\mathrm{L1}} & 0 \\ 0 & 0 & A_{\mathrm{L2f}} & A_{\mathrm{L2p}} & A_{\mathrm{L4f}} & A_{\mathrm{L4p}} & 0 & U_{\mathrm{L2}} \end{bmatrix} \tag{6}$$

$$\boldsymbol{A}^{\cdot\mathrm{p}}_{\mathrm{b}} = \begin{bmatrix} A_{\mathrm{T1f}} & A_{\mathrm{T1p}} & 0 & 0 & 0 & 0 & 0 & 0 \\ 0 & 0 & A_{\mathrm{T2f}} & A_{\mathrm{T2p}} & 0 & 0 & 0 & 0 \\ 0 & 0 & 0 & 0 & A_{\mathrm{TRf}} & A_{\mathrm{TRp}} & 0 & 0 \\ A_{\mathrm{L1f}} & A_{\mathrm{L1p}} & 0 & 0 & 0 & 0 & U_{\mathrm{L1}} & 0 \\ 0 & 0 & A_{\mathrm{L2f}} & A_{\mathrm{L2p}} & 0 & 0 & 0 & U_{\mathrm{L2}} \end{bmatrix} \tag{7}$$

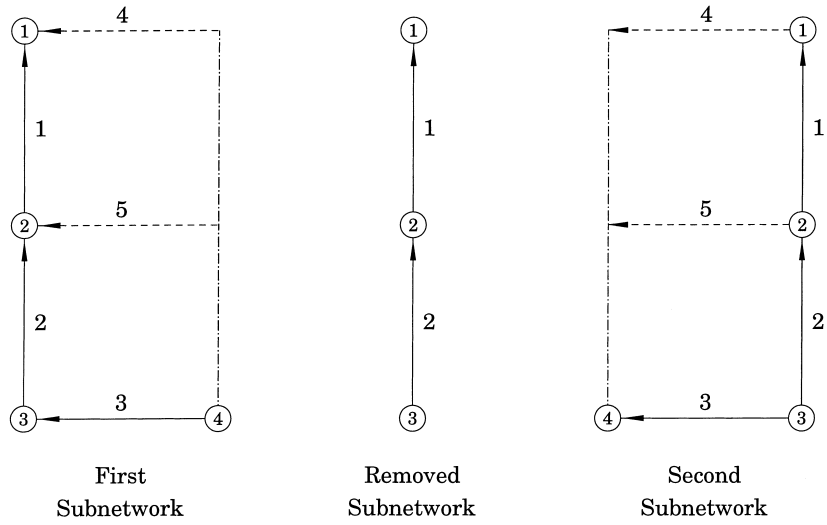

Fig. 3. Torn configuration of network SIMP cut by mesh diakoptics.

$$\boldsymbol{C}^{\mathrm{b}}_{.\mathrm{s}} = \begin{bmatrix} B_{\mathrm{T1f}} & B_{\mathrm{T1p}} & 0 & 0 & 0 & 0 & C_{\mathrm{T1}} & 0 \\ 0 & 0 & B_{\mathrm{T2f}} & B_{\mathrm{T2p}} & 0 & 0 & 0 & C_{\mathrm{T2}} \\ 0 & 0 & 0 & 0 & B_{\mathrm{TRf}} & B_{\mathrm{TRp}} & C_{\mathrm{T3}} & C_{\mathrm{T4}} \\ 0 & 0 & 0 & 0 & 0 & 0 & U_{\mathrm{L1}} & 0 \\ 0 & 0 & 0 & 0 & 0 & 0 & 0 & U_{\mathrm{L2}} \end{bmatrix} \tag{8}$$

$$\boldsymbol{C}^{\mathrm{b}}_{.\mathrm{p}} = \begin{bmatrix} B_{\mathrm{T1f}} & B_{\mathrm{T1p}} & 0 & 0 & 0 & 0 & C_{\mathrm{T1}} & 0 \\ 0 & 0 & B_{\mathrm{T2f}} & B_{\mathrm{T2p}} & 0 & 0 & 0 & C_{\mathrm{T2}} \\ 0 & 0 & 0 & 0 & B_{\mathrm{TRf}} & B_{\mathrm{TRp}} & 0 & 0 \\ 0 & 0 & 0 & 0 & 0 & 0 & U_{\mathrm{L1}} & 0 \\ 0 & 0 & 0 & 0 & 0 & 0 & 0 & U_{\mathrm{L2}} \end{bmatrix} \tag{9}$$

$$\boldsymbol{C}^{\mathrm{s}}_{.\mathrm{p}} = \boldsymbol{A}^{\mathrm{s}}_{\mathrm{b}}\boldsymbol{C}^{\mathrm{b}}_{.\mathrm{p}} = \begin{bmatrix} U_{\mathrm{T1f}} & 0 & 0 & 0 & 0 & 0 & 0 & 0 \\ 0 & U_{\mathrm{T1p}} & 0 & 0 & 0 & 0 & 0 & 0 \\ 0 & 0 & U_{\mathrm{T2f}} & 0 & 0 & 0 & 0 & 0 \\ 0 & 0 & 0 & U_{\mathrm{T2p}} & 0 & 0 & 0 & 0 \\ 0 & 0 & 0 & 0 & U_{\mathrm{TRf}} & 0 & \overline{A_{\mathrm{L3f}}} & \overline{A_{\mathrm{L4f}}} \\ 0 & 0 & 0 & 0 & 0 & U_{\mathrm{TRp}} & \overline{A_{\mathrm{L3p}}} & \overline{A_{\mathrm{L4p}}} \\ 0 & 0 & 0 & 0 & 0 & 0 & U_{\mathrm{L1}} & 0 \\ 0 & 0 & 0 & 0 & 0 & 0 & 0 & U_{\mathrm{L2}} \end{bmatrix} \tag{10}$$

$$\boldsymbol{A}^{\mathrm{p}}_{.\mathrm{s}} = \boldsymbol{A}^{\mathrm{p}}_{\mathrm{b}}\boldsymbol{C}^{\mathrm{b}}_{.\mathrm{s}} = \begin{bmatrix} U_{\mathrm{T1f}} & 0 & 0 & 0 & 0 & 0 & 0 & 0 \\ 0 & U_{\mathrm{T1p}} & 0 & 0 & 0 & 0 & 0 & 0 \\ 0 & 0 & U_{\mathrm{T2f}} & 0 & 0 & 0 & 0 & 0 \\ 0 & 0 & 0 & U_{\mathrm{T2p}} & 0 & 0 & 0 & 0 \\ 0 & 0 & 0 & 0 & U_{\mathrm{TRf}} & 0 & \overline{A_{\mathrm{TRf}}}C_{\mathrm{T3}} & \overline{A_{\mathrm{L4f}}}C_{\mathrm{T4}} \\ 0 & 0 & 0 & 0 & 0 & U_{\mathrm{TRp}} & \overline{A_{\mathrm{L3p}}}C_{\mathrm{T3}} & \overline{A_{\mathrm{L4p}}}C_{\mathrm{T4}} \\ 0 & 0 & 0 & 0 & 0 & 0 & U_{\mathrm{L1}} & 0 \\ 0 & 0 & 0 & 0 & 0 & 0 & 0 & U_{\mathrm{L2}} \end{bmatrix} \tag{11}$$

Using the equation based on Ohm's law and applying the relevant transformation:

$$\boldsymbol{V}_{\mathrm{p}} = \boldsymbol{C}^{.\mathrm{b}}_{\mathrm{p}}\boldsymbol{Z}_{\mathrm{bb}}\boldsymbol{C}^{\mathrm{b}}_{.\mathrm{p}}\boldsymbol{J}^{\mathrm{p}} \tag{12}$$

Expanding Eq. (12) in matrix form:

$$\begin{bmatrix} V^*_{\mathrm{T1f}} \\ V^*_{\mathrm{T1p}} \\ V^*_{\mathrm{T2f}} \\ V^*_{\mathrm{T2p}} \\ V^*_{\mathrm{TRf}} \\ V^*_{\mathrm{TRp}} \\ V^*_{\mathrm{L1}} \\ V^*_{\mathrm{L2}} \end{bmatrix} = \begin{bmatrix} \overline{B_{\mathrm{T1f}}}Z_{\mathrm{T1}}B_{\mathrm{T1f}}I^*_{\mathrm{1f}} + \overline{B_{\mathrm{T1f}}}Z_{\mathrm{T1}}B_{\mathrm{T1p}}I^*_{\mathrm{1p}} + \overline{B_{\mathrm{T1f}}}Z_{\mathrm{T1}}C_{\mathrm{T1}}i^*_1 \\ \overline{B_{\mathrm{T1p}}}Z_{\mathrm{T1}}B_{\mathrm{T1f}}I^*_{\mathrm{1f}} + \overline{B_{\mathrm{T1p}}}Z_{\mathrm{T1}}B_{\mathrm{T1p}}I^*_{\mathrm{1p}} + \overline{B_{\mathrm{T1p}}}Z_{\mathrm{T1}}C_{\mathrm{T1}}i^*_1 \\ \overline{B_{\mathrm{T2f}}}Z_{\mathrm{T2}}B_{\mathrm{T2f}}I^*_{\mathrm{2f}} + \overline{B_{\mathrm{T2f}}}Z_{\mathrm{T2}}B_{\mathrm{T2p}}I^*_{\mathrm{2p}} + \overline{B_{\mathrm{T2f}}}Z_{\mathrm{T2}}C_{\mathrm{T2}}i^*_2 \\ \overline{B_{\mathrm{T2p}}}Z_{\mathrm{T2}}B_{\mathrm{T2f}}I^*_{\mathrm{2f}} + \overline{B_{\mathrm{T2p}}}Z_{\mathrm{T2}}B_{\mathrm{T2p}}I^*_{\mathrm{2p}} + \overline{B_{\mathrm{T2p}}}Z_{\mathrm{T2}}C_{\mathrm{T2}}i^*_2 \\ \overline{B_{\mathrm{TRf}}}Z_{\mathrm{TR}}B_{\mathrm{TRf}}I^*_{\mathrm{Rf}} + \overline{B_{\mathrm{TRf}}}Z_{\mathrm{TR}}B_{\mathrm{TRp}}I^*_{\mathrm{Rp}} \\ \overline{B_{\mathrm{TRp}}}Z_{\mathrm{TR}}B_{\mathrm{TRf}}I^*_{\mathrm{Rf}} + \overline{B_{\mathrm{TRp}}}Z_{\mathrm{TR}}B_{\mathrm{TRp}}I^*_{\mathrm{Rp}} \\ (\overline{C_{\mathrm{T1}}}Z_{\mathrm{T1}}C_{\mathrm{T1}} + Z_{\mathrm{L1}})i^*_1 + \overline{C_{\mathrm{T1}}}Z_{\mathrm{T1}}B_{\mathrm{T1f}}I^*_{\mathrm{1f}} + \overline{C_{\mathrm{T1}}}Z_{\mathrm{T1}}B_{\mathrm{T1p}}I^*_{\mathrm{1p}} \\ (\overline{C_{\mathrm{T2}}}Z_{\mathrm{T2}}C_{\mathrm{T2}} + Z_{\mathrm{L2}})i^*_2 + \overline{C_{\mathrm{T2}}}Z_{\mathrm{T2}}B_{\mathrm{T2f}}I^*_{\mathrm{2f}} + \overline{C_{\mathrm{T2}}}Z_{\mathrm{T2}}B_{\mathrm{T2p}}I^*_{\mathrm{2p}} \end{bmatrix} \tag{13}$$

$$\begin{bmatrix} V^*_{\mathrm{T1f}} \\ V^*_{\mathrm{T1p}} \\ V^*_{\mathrm{T2f}} \\ V^*_{\mathrm{T2p}} \\ V^*_{\mathrm{TRf}} \\ V^*_{\mathrm{TRp}} \\ V^*_{\mathrm{L1}} \\ V^*_{\mathrm{L2}} \end{bmatrix} = \begin{bmatrix} Z^*_{\mathrm{T1f}} & 0 & 0 & 0 & 0 & 0 & 0 & 0 \\ 0 & Z^*_{\mathrm{T1p}} & 0 & 0 & 0 & 0 & 0 & 0 \\ 0 & 0 & Z^*_{\mathrm{T2f}} & 0 & 0 & 0 & 0 & 0 \\ 0 & 0 & 0 & Z^*_{\mathrm{T2p}} & 0 & 0 & 0 & 0 \\ 0 & 0 & 0 & 0 & Z^*_{\mathrm{TRf}} & 0 & 0 & 0 \\ 0 & 0 & 0 & 0 & 0 & Z^*_{\mathrm{TRp}} & 0 & 0 \\ 0 & 0 & 0 & 0 & 0 & 0 & Z^*_{\mathrm{L1}} & 0 \\ 0 & 0 & 0 & 0 & 0 & 0 & 0 & Z^*_{\mathrm{L2}} \end{bmatrix} \begin{bmatrix} I^*_{\mathrm{1f}} \\ I^*_{\mathrm{1p}} \\ I^*_{\mathrm{2f}} \\ I^*_{\mathrm{2p}} \\ I^*_{\mathrm{Rf}} \\ I^*_{\mathrm{Rp}} \\ i^*_1 \\ i^*_2 \end{bmatrix} + \begin{bmatrix} \overline{B_{\mathrm{T1f}}}Z_{\mathrm{T1}}B_{\mathrm{T1p}}I^*_{\mathrm{1p}} + \overline{B_{\mathrm{T1f}}}Z_{\mathrm{T1}}C_{\mathrm{T1}}i^*_1 \\ \overline{B_{\mathrm{T1p}}}Z_{\mathrm{T1}}B_{\mathrm{T1f}}I^*_{\mathrm{1f}} + \overline{B_{\mathrm{T1p}}}Z_{\mathrm{T1}}C_{\mathrm{T1}}i^*_1 \\ \overline{B_{\mathrm{T2f}}}Z_{\mathrm{T2}}B_{\mathrm{T2p}}I^*_{\mathrm{2p}} + \overline{B_{\mathrm{T2f}}}Z_{\mathrm{T2}}C_{\mathrm{T2}}i^*_2 \\ \overline{B_{\mathrm{T2p}}}Z_{\mathrm{T2}}B_{\mathrm{T2f}}I^*_{\mathrm{2f}} + \overline{B_{\mathrm{T2p}}}Z_{\mathrm{T2}}C_{\mathrm{T2}}i^*_2 \\ \overline{B_{\mathrm{TRf}}}Z_{\mathrm{TR}}B_{\mathrm{TRp}}I^*_{\mathrm{Rp}} \\ \overline{B_{\mathrm{TRp}}}Z_{\mathrm{TR}}B_{\mathrm{TRf}}I^*_{\mathrm{Rf}} \\ \overline{C_{\mathrm{T1}}}Z_{\mathrm{T1}}B_{\mathrm{T1f}}I^*_{\mathrm{1f}} + \overline{C_{\mathrm{T1}}}Z_{\mathrm{T1}}B_{\mathrm{T1p}}I^*_{\mathrm{1p}} \\ \overline{C_{\mathrm{T2}}}Z_{\mathrm{T2}}B_{\mathrm{T2f}}I^*_{\mathrm{2f}} + \overline{C_{\mathrm{T2}}}Z_{\mathrm{T2}}B_{\mathrm{T2p}}I^*_{\mathrm{2p}} \end{bmatrix} \tag{14}$$

where

$$Z^*_{\mathrm{T1f}} = \overline{B_{\mathrm{T1f}}}\,Z_{\mathrm{T1}}\,B_{\mathrm{T1f}} \tag{15a}$$

$$Z^*_{\mathrm{T1p}} = \overline{B_{\mathrm{T1p}}}\,Z_{\mathrm{T1}}\,B_{\mathrm{T1p}} \tag{15b}$$

$$Z^*_{\mathrm{T2f}} = \overline{B_{\mathrm{T2f}}}\,Z_{\mathrm{T2}}\,B_{\mathrm{T2f}} \tag{15c}$$

$$Z^*_{\mathrm{T2p}} = \overline{B_{\mathrm{T2p}}}\,Z_{\mathrm{T2}}\,B_{\mathrm{T2p}} \tag{15d}$$

$$Z^*_{\mathrm{TRf}} = \overline{B_{\mathrm{TRf}}}\,Z_{\mathrm{TR}}\,B_{\mathrm{TRf}} \tag{15e}$$

$$Z^*_{TRp} = \overline{B_{TRp}}\, Z_{TR}\, B_{TRp} \tag{15f}$$

$$Z^*_{L1} = \overline{C_{T1}}\, Z_{T1}\, C_{T1} + Z_{L1} \tag{15g}$$

$$Z^*_{L2} = \overline{C_{T2}}\, Z_{T2}\, C_{T2} + Z_{L2} \tag{15h}$$

Rearranging Eq. (14),

$$\begin{bmatrix} I^*_{1f} \\ I^*_{1p} \\ I^*_{2f} \\ I^*_{2p} \\ I^*_{Rf} \\ I^*_{Rp} \\ i^*_1 \\ i^*_2 \end{bmatrix} = \begin{bmatrix} Z^{*-1}_{T1f} & 0 & 0 & 0 & 0 & 0 & 0 & 0 \\ 0 & Z^{*-1}_{T1p} & 0 & 0 & 0 & 0 & 0 & 0 \\ 0 & 0 & Z^{*-1}_{T2f} & 0 & 0 & 0 & 0 & 0 \\ 0 & 0 & 0 & Z^{*-1}_{T2p} & 0 & 0 & 0 & 0 \\ 0 & 0 & 0 & 0 & Z^{*-1}_{TRf} & 0 & 0 & 0 \\ 0 & 0 & 0 & 0 & 0 & Z^{*-1}_{TRp} & 0 & 0 \\ 0 & 0 & 0 & 0 & 0 & 0 & Z^{*-1}_{L1} & 0 \\ 0 & 0 & 0 & 0 & 0 & 0 & 0 & Z^{*-1}_{L2} \end{bmatrix} \times \begin{bmatrix} V^*_{T1f} - \overline{B_{T1f}} Z_{T1} B_{T1p} I^*_{1p} + \overline{B_{T1f}} Z_{T1} C_{T1} i^*_1 \\ V^*_{T1p} - \overline{B_{T1p}} Z_{T1} B_{T1f} I^*_{1f} + \overline{B_{T1p}} Z_{T1} C_{T1} i^*_1 \\ V^*_{T2f} - \overline{B_{T2f}} Z_{T2} B_{T2p} I^*_{2p} + \overline{B_{T2f}} Z_{T2} C_{T2} i^*_2 \\ V^*_{T2p} - \overline{B_{T2p}} Z_{T2} B_{T2f} I^*_{2f} + \overline{B_{T2p}} Z_{T2} C_{T2} i^*_2 \\ V^*_{Trf} - \overline{B_{TRf}} Z_{TR} B_{TRp} I^*_{Rp} \\ V^*_{TRp} - \overline{B_{TRp}} Z_{TR} B_{TRf} I^*_{Rf} \\ V^*_{L1} - \overline{C_{T1}} Z_{T1} B_{T1f} I^*_{1f} + \overline{C_{T1}} Z_{T1} B_{T1p} I^*_{1p} \\ V^*_{L2} - \overline{C_{T2}} Z_{T2} B_{T2f} I^*_{2f} + \overline{C_{T2}} Z_{T2} B_{T2p} I^*_{2p} \end{bmatrix} \tag{16}$$

Transforming both flow and pressure in Eq. (16) from the torn framework to the ovthogonal framework using Eqs. (2), (5) and (10).

$$I_{1f} = Z^{*-1}_{T1f}(V_{T1f} - \overline{B_{T1f}} Z_{T1} B_{T1p} I_{1p} - \overline{B_{T1f}} Z_{T1} C_{T1} i_1) \tag{17a}$$

$$I_{1p} = Z^{*-1}_{T1p}(V_{T1p} - \overline{B_{T1p}} Z_{T1} B_{T1f} I_{1f} - \overline{B_{T1p}} Z_{T1} C_{T1} i_1) \tag{17b}$$

$$I_{2f} = Z^{*-1}_{T2f}(V_{T2f} - \overline{B_{T2f}} Z_{T2} B_{T2p} I_{2p} - \overline{B_{T2f}} Z_{T2} C_{T2} i_2) \tag{17c}$$

$$I_{2p} = Z^{*-1}_{T2p}(V_{T2p} - \overline{B_{T2p}} Z_{T2} B_{T2f} I_{2f} - \overline{B_{T2p}} Z_{T2} C_{T2} i_2) \tag{17d}$$

$$i_1 = Z^{*-1}_{L1}(A_{L3f} V_{TRf} + A_{L3p} V_{TRp} + V_{L1} - \overline{C_{T1}} Z_{T1} B_{T1f} I_{1f} - \overline{C_{T1}} Z_{T1} B_{T1p} I_{1p}) \tag{17e}$$

$$i_2 = Z^{*-1}_{L2}(A_{L4f} V_{TRf} + A_{L4p} V_{TRp} + V_{L2} - \overline{C_{T2}} Z_{T2} B_{T2f} I_{2f} - \overline{C_{T2}} Z_{T2} B_{T2f} I_{2p}) \tag{17f}$$

$$I_{Rf} = Z^{*-1}_{TRf}[V_{TRf} - \overline{B_{TRf}} Z_{TR} B_{TRp}(I_{Rp} + \overline{A_{TRp}} C_{T3} i_1 + \overline{A_{TRp}} C_{T4} i_2)] + \overline{A_{L3f}} i_1 + \overline{A_{L4f}} i_2 \tag{17g}$$

$$I_{Rp} = Z^{*-1}_{TRp}[V_{TRp} - \overline{B_{TRp}} Z_{TR} B_{TRf}(I_{Rf} + \overline{A_{TRf}} C_{T3} i_1 + \overline{A_{TRf}} C_{T4} i_2)] + \overline{A_{L3p}} i_1 + \overline{A_{L4p}} i_2 \tag{17h}$$

Eqs. (17a–h), form the set of eight working equations which are solved simultaneously to obtain the eight unknown quantities: i_1, i_2, I_{1p}, I_{2p}, I_{Rp}, V_{T1f}, V_{T2f} and V_{TRf}.

The solution strategy for solving the eight equations are given in the steps below:

(a) From Eqs. (17g) and (17h) express I_{Rp} and V_{TRf} in terms of i_1 and i_2;
(b) Substitute for I_{1p} and I_{2p} from Eqs. (17b) and (17d) into Eqs. (17e) and (17f) to get two equations involving i_1 and i_2 which are then solved;
(c) With i_1 and i_2 found, determine V_{T1f} and V_{T2f} from equations Eqs. (17a) and (17c) respectively;
(d) Obtain I_{1p} and I_{2p} from Eqs. (17b) and (17d) respectively;
(e) Calculate I_{Rp} and V_{TRf} from the equations obtained in step (a).

3.2. Nodal partitioning diakoptics

In nodal diakoptics, the given network is torn in such a way that the removed subnetwork consists only of link with no nodes and no tree branches. For instance, the network SIMP in Fig. 1 may be cut by nodal diakoptics in the manner shown in Fig. 4 and the resulting torn configuration is represented in Fig. 5. In the derivation of this method, most of the tensors to be inverted are of the order of the non-datum nodes of subnetworks. Moreover, the formulation of this method employs a fundamental equation essentially similar to that for nodal partitioning, hence the name nodal partitioning diakoptics.

The relevant tensors are given below:

$$\boldsymbol{A}^{s}_{b} = \begin{bmatrix} A_{T1f} & A_{T1p} & 0 & 0 & 0 & 0 & 0 \\ 0 & 0 & A_{T2f} & A_{T2p} & 0 & 0 & 0 \\ A_{L1f} & A_{L1p} & 0 & 0 & U_{L1} & 0 & 0 \\ 0 & 0 & A_{L2f} & A_{L2p} & 0 & U_{L2} & 0 \\ A_{L3f} & A_{L3p} & A_{L4f} & A_{L4p} & 0 & 0 & U_{LR} \end{bmatrix} \tag{18}$$

$$\boldsymbol{A}^{p}_{b} = \begin{bmatrix} A_{T1f} & A_{T1p} & 0 & 0 & 0 & 0 & 0 \\ 0 & 0 & A_{T2f} & A_{T2p} & 0 & 0 & 0 \\ A_{L1f} & A_{L1p} & 0 & 0 & U_{L1} & 0 & 0 \\ 0 & 0 & A_{L2f} & A_{L2p} & 0 & U_{L2} & 0 \\ 0 & 0 & 0 & 0 & 0 & 0 & U_{LR} \end{bmatrix} \tag{19}$$

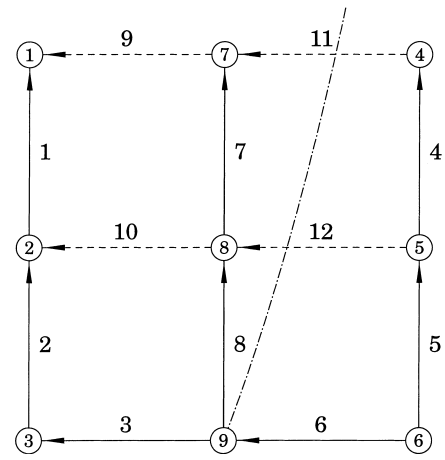

Fig. 4. Network SIMP cut by nodal diakoptics.

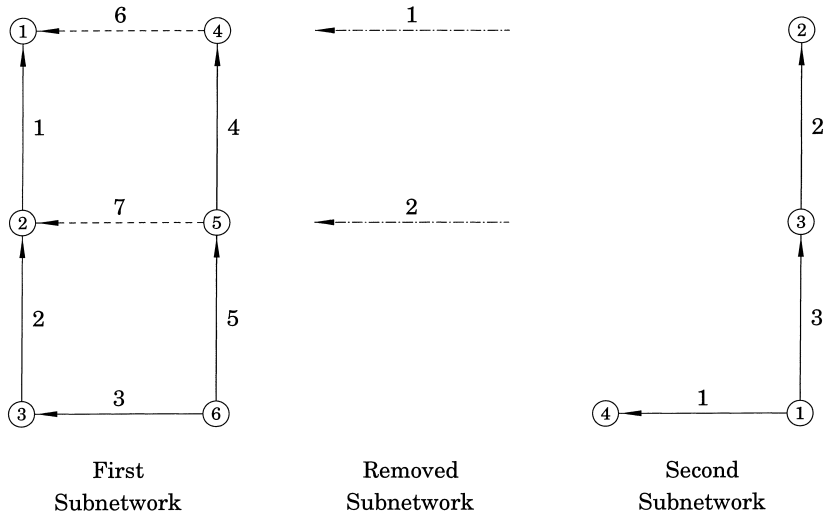

Fig. 5. Torn configuration of network SIMP cut by nodal diakoptics.

$$\boldsymbol{C}^{\mathrm{b}}_{.\mathrm{s}} = \begin{bmatrix} B_{\mathrm{T1f}} & B_{\mathrm{T1p}} & 0 & 0 & C_{\mathrm{T1}} & 0 & C_{\mathrm{T3}} \\ 0 & 0 & B_{\mathrm{T2f}} & B_{\mathrm{T2p}} & 0 & C_{\mathrm{T2}} & C_{\mathrm{T4}} \\ 0 & 0 & 0 & 0 & U_{\mathrm{L1}} & 0 & 0 \\ 0 & 0 & 0 & 0 & 0 & U_{\mathrm{L2}} & 0 \\ 0 & 0 & 0 & 0 & 0 & 0 & U_{\mathrm{LR}} \end{bmatrix} \tag{20}$$

Using the equation based on Ohm's law and applying the relevant transformation:

$$\boldsymbol{J}^{\mathrm{p}} = \boldsymbol{A}^{\mathrm{p}}_{.\mathrm{b}} \boldsymbol{Y}^{\mathrm{bb}} \boldsymbol{A}^{.\mathrm{p}}_{\mathrm{b}} \boldsymbol{V}_{\mathrm{p}} \tag{24a}$$

Expanding Eq. (24a) in matrix form:

$$\begin{bmatrix} I^*_{\mathrm{1f}} \\ I^*_{\mathrm{1p}} \\ I^*_{\mathrm{2f}} \\ I^*_{\mathrm{2p}} \\ i^*_1 \\ i^*_2 \\ i^*_{\mathrm{R}} \end{bmatrix} = \begin{bmatrix} (\overline{A_{\mathrm{T1f}}} Y_{\mathrm{T1}} A_{\mathrm{T1f}} + \overline{A_{\mathrm{L1f}}} Y_{\mathrm{L1}} A_{\mathrm{L1f}}) V^*_{\mathrm{T1f}} + (\overline{A_{\mathrm{T1f}}} Y_{\mathrm{T1}} A_{\mathrm{T1p}} + \overline{A_{\mathrm{L1f}}} Y_{\mathrm{L1}} A_{\mathrm{L1p}}) V^*_{\mathrm{T1p}} + \overline{A_{\mathrm{L1f}}} Y_{\mathrm{L1}} A^*_{\mathrm{L1}} \\ (\overline{A_{\mathrm{T1p}}} Y_{\mathrm{T1}} A_{\mathrm{T1f}} + \overline{A_{\mathrm{L1p}}} Y_{\mathrm{L1}} A_{\mathrm{L1f}}) V^*_{\mathrm{T1f}} + (\overline{A_{\mathrm{T1p}}} Y_{\mathrm{T1}} A_{\mathrm{T1p}} + \overline{A_{\mathrm{L1p}}} Y_{\mathrm{L1}} A_{\mathrm{L1p}}) V^*_{\mathrm{T1p}} + \overline{A_{\mathrm{L1p}}} Y_{\mathrm{L1}} V^*_{\mathrm{L1}} \\ (\overline{A_{\mathrm{T2f}}} Y_{\mathrm{T2}} A_{\mathrm{T2f}} + \overline{A_{\mathrm{L2f}}} Y_{\mathrm{L2}} A_{\mathrm{L2f}}) V^*_{\mathrm{T2f}} + (\overline{A_{\mathrm{T2f}}} Y_{\mathrm{T2}} A_{\mathrm{T2p}} + \overline{A_{\mathrm{L2f}}} Y_{\mathrm{L2}} A_{\mathrm{L2p}}) V^*_{\mathrm{T2p}} + \overline{A_{\mathrm{L2f}}} Y_{\mathrm{L2}} V^*_{\mathrm{L2}} \\ (\overline{A_{\mathrm{T2p}}} Y_{\mathrm{T2}} A_{\mathrm{T2f}} + \overline{A_{\mathrm{L2p}}} Y_{\mathrm{L2}} A_{\mathrm{L2f}}) V^*_{\mathrm{T2f}} + (\overline{A_{\mathrm{T2p}}} Y_{\mathrm{T2}} A_{\mathrm{T2p}} + \overline{A_{\mathrm{L2p}}} Y_{\mathrm{L2}} A_{\mathrm{L2p}}) V^*_{\mathrm{T2p}} + \overline{A_{\mathrm{L2p}}} Y_{\mathrm{L2}} V^*_{\mathrm{L2}} \\ Y_{\mathrm{L1}} V^*_{\mathrm{L1}} + Y_{\mathrm{L1}} A_{\mathrm{L1f}} V^*_{\mathrm{T1f}} + Y_{\mathrm{L1}} A_{\mathrm{L1p}} V^*_{\mathrm{T1p}} \\ Y_{\mathrm{L2}} V^*_{\mathrm{L2}} + Y_{\mathrm{L2}} A_{\mathrm{L2f}} V^*_{\mathrm{T2f}} + Y_{\mathrm{L2}} A_{\mathrm{L2p}} V^*_{\mathrm{T2p}} \\ Y_{\mathrm{LR}} V^*_{\mathrm{LR}} \end{bmatrix} \tag{24b}$$

$$\boldsymbol{C}^{\mathrm{b}}_{.\mathrm{p}} = \begin{bmatrix} B_{\mathrm{T1f}} & B_{\mathrm{T1p}} & 0 & 0 & C_{\mathrm{T1}} & 0 & 0 \\ 0 & 0 & B_{\mathrm{T2f}} & B_{\mathrm{T2p}} & 0 & C_{\mathrm{T2}} & 0 \\ 0 & 0 & 0 & 0 & U_{\mathrm{L1}} & 0 & 0 \\ 0 & 0 & 0 & 0 & 0 & U_{\mathrm{L2}} & 0 \\ 0 & 0 & 0 & 0 & 0 & 0 & U_{\mathrm{L2}} \end{bmatrix} \tag{21}$$

$$\boldsymbol{A}^{\mathrm{p}}_{.\mathrm{s}} = \boldsymbol{A}^{\mathrm{p}}_{.\mathrm{b}} \boldsymbol{C}^{\mathrm{b}}_{.\mathrm{s}} = \begin{bmatrix} U_{\mathrm{T1f}} & 0 & 0 & 0 & 0 & 0 & 0 \\ 0 & U_{\mathrm{T1p}} & 0 & 0 & 0 & 0 & 0 \\ 0 & 0 & U_{\mathrm{T2f}} & 0 & 0 & 0 & 0 \\ 0 & 0 & 0 & U_{\mathrm{T2p}} & 0 & 0 & 0 \\ 0 & 0 & 0 & 0 & U_{\mathrm{L1}} & 0 & 0 \\ 0 & 0 & 0 & 0 & 0 & U_{\mathrm{L2}} & 0 \\ \overline{C_{\mathrm{T3}}} A_{\mathrm{T1f}} & \overline{C_{\mathrm{T3}}} A_{\mathrm{T1P}} & \overline{C_{\mathrm{T4}}} A_{\mathrm{T2F}} & \overline{C_{\mathrm{T4}}} A_{\mathrm{T2p}} & 0 & 0 & U_{\mathrm{LR}} \end{bmatrix} \tag{22}$$

$$\boldsymbol{C}^{\mathrm{s}}_{.\mathrm{p}} = \boldsymbol{A}^{\mathrm{s}}_{.\mathrm{b}} \boldsymbol{C}^{\mathrm{b}}_{.\mathrm{p}} = \begin{bmatrix} U_{\mathrm{T1f}} & 0 & 0 & 0 & 0 & 0 & \overline{A_{\mathrm{L3f}}} \\ 0 & U_{\mathrm{T1p}} & 0 & 0 & 0 & 0 & \overline{A_{\mathrm{L3P}}} \\ 0 & 0 & U_{\mathrm{T2f}} & 0 & 0 & 0 & \overline{A_{\mathrm{L4f}}} \\ 0 & 0 & 0 & U_{\mathrm{T2p}} & 0 & 0 & \overline{A_{\mathrm{L4P}}} \\ 0 & 0 & 0 & 0 & U_{\mathrm{L1}} & 0 & 0 \\ 0 & 0 & 0 & 0 & 0 & U_{\mathrm{L2}} & 0 \\ 0 & 0 & 0 & 0 & 0 & 0 & U_{\mathrm{LR}} \end{bmatrix} \tag{23}$$

$$\begin{bmatrix} I^*_{\mathrm{1f}} \\ I^*_{\mathrm{1p}} \\ I^*_{\mathrm{2f}} \\ I^*_{\mathrm{2p}} \\ i^*_1 \\ i^*_2 \\ i^*_R \end{bmatrix} = \begin{bmatrix} Y_{\mathrm{T1f}^*} & 0 & 0 & 0 & 0 & 0 & 0 \\ 0 & Y^*_{\mathrm{T1p}} & 0 & 0 & 0 & 0 & 0 \\ 0 & 0 & Y^*_{\mathrm{T2f}} & 0 & 0 & 0 & 0 \\ 0 & 0 & 0 & Y^*_{\mathrm{T2p}} & 0 & 0 & 0 \\ 0 & 0 & 0 & 0 & Y^*_{\mathrm{L1}} & 0 & 0 \\ 0 & 0 & 0 & 0 & 0 & Y^*_{\mathrm{L2}} & 0 \\ 0 & 0 & 0 & 0 & 0 & 0 & Y^*_{\mathrm{LR}} \end{bmatrix} \begin{bmatrix} V^*_{\mathrm{T1f}} \\ V^*_{\mathrm{T1p}} \\ V^*_{\mathrm{T2f}} \\ V^*_{\mathrm{T2p}} \\ V^*_{\mathrm{L1}} \\ V^*_{\mathrm{L2}} \\ V^*_{\mathrm{LR}} \end{bmatrix}$$

$$\times \begin{bmatrix} (\overline{A_{\mathrm{T1f}}} Y_{\mathrm{T1}} A_{\mathrm{T1p}} + \overline{A_{\mathrm{L1f}}} Y_{\mathrm{L1}} A_{\mathrm{L1p}}) V^*_{\mathrm{T1p}} + \overline{A_{\mathrm{L1f}}} Y_{\mathrm{L1}} V^*_{\mathrm{L1}} \\ (\overline{A_{\mathrm{T1p}}} Y_{\mathrm{T1}} A_{\mathrm{T1f}} + \overline{A_{\mathrm{L1p}}} Y_{\mathrm{L1}} A_{\mathrm{L1f}}) V^*_{\mathrm{T1f}} + \overline{A_{\mathrm{L1p}}} Y_{\mathrm{L1}} V^*_{\mathrm{L1}} \\ (\overline{A_{\mathrm{T2f}}} Y_{\mathrm{T2}} A_{\mathrm{T2p}} + \overline{A_{\mathrm{L2f}}} Y_{\mathrm{L2}} A_{\mathrm{L2p}}) V^*_{\mathrm{T2p}} + \overline{A_{\mathrm{L2f}}} Y_{\mathrm{L2}} V^*_{\mathrm{L2}} \\ (\overline{A_{\mathrm{T2p}}} Y_{\mathrm{T2}} A_{\mathrm{T2f}} + \overline{A_{\mathrm{L2p}}} Y_{\mathrm{L2}} A_{\mathrm{L2f}}) V^*_{\mathrm{T2f}} + \overline{A_{\mathrm{L2p}}} Y_{\mathrm{L2}} V^*_{\mathrm{L2}} \\ Y_{\mathrm{L1}} A_{\mathrm{L1f}} V^*_{\mathrm{T1f}} + Y_{\mathrm{L1}} A_{\mathrm{L1p}} V_{\mathrm{T1p}^*} \\ Y_{\mathrm{L2}} A_{\mathrm{L2f}} V^*_{\mathrm{T2f}} + Y_{\mathrm{L2}} A_{\mathrm{L2p}} V^*_{\mathrm{T2p}} \\ 0 \end{bmatrix} \tag{25}$$

where

$$Y^*_{\mathrm{T1f}} = \overline{A_{\mathrm{T1f}}} Y_{\mathrm{T1}} A_{\mathrm{T1f}} + \overline{A_{\mathrm{L1f}}} Y_{\mathrm{L1}} A_{\mathrm{L1f}} \tag{26a}$$

$$Y^*_{T1p} = \overline{A_{T1p}} Y_{T1} A_{T1p} + \overline{A_{L1p}} Y_{L1} A_{L1p} \quad (26b)$$

$$Y^*_{T2f} = \overline{A_{T2f}} Y_{T1} A_{T2f} + \overline{A_{L2f}} Y_{L1} A_{L2f} \quad (26c)$$

$$Y^*_{T2p} = \overline{A_{T2p}} Y_{T1} A_{T2p} + \overline{A_{L2p}} Y_{L1} A_{L2p} \quad (26d)$$

$$Y^*_{L1} = Y_{L1} \quad (26e)$$

$$Y^*_{L2} = Y_{L2} \quad (26f)$$

$$Y^*_{LR} = Y_{LR} \quad (26g)$$

Re-arranging Eq. (25),

$$\begin{bmatrix} V^*_{T1f} \\ V^*_{T1p} \\ V^*_{T2f} \\ V^*_{T2p} \\ V^*_{L1} \\ V^*_{L2} \\ V^*_{LR} \end{bmatrix} = \begin{bmatrix} Y^{*-1}_{T1f} & 0 & 0 & 0 & 0 & 0 & 0 \\ 0 & Y^{*-1}_{T1p} & 0 & 0 & 0 & 0 & 0 \\ 0 & 0 & Y^{*-1}_{T2f} & 0 & 0 & 0 & 0 \\ 0 & 0 & 0 & Y^{*-1}_{T2p} & 0 & 0 & 0 \\ 0 & 0 & 0 & 0 & Y^{*-1}_{L1} & 0 & 0 \\ 0 & 0 & 0 & 0 & 0 & Y^{*-1}_{L2} & 0 \\ 0 & 0 & 0 & 0 & 0 & 0 & Y^{*-1}_{LR} \end{bmatrix}$$

$$\times \left[\begin{bmatrix} I^*_{1f} \\ I^*_{1p} \\ I^*_{2f} \\ I^*_{2p} \\ i^*_1 \\ i^*_2 \\ i^*_R \end{bmatrix} - \begin{bmatrix} (\overline{A_{T1f}} Y_{T1} A_{T1p} + \overline{A_{L1f}} Y_{L1} A_{L1p}) V^*_{T1p} + \overline{A_{L1f}} Y_{L1} V^*_{L1} \\ (\overline{A_{T1p}} Y_{T1} A_{T1f} + \overline{A_{L1p}} Y_{L1} A_{L1f}) V^*_{T1f} + \overline{A_{L1p}} Y_{L1} V^*_{L1} \\ (\overline{A_{T2f}} Y_{T2} A_{T2p} + \overline{A_{L2f}} Y_{L2} A_{L2p}) V^*_{T2p} + \overline{A_{L2f}} Y_{L2} V^*_{L2} \\ (\overline{A_{T2p}} Y_{T2} A_{T2f} + \overline{A_{L2p}} Y_{L2} A_{L2f}) V^*_{T2f} + \overline{A_{L2p}} Y_{L2} V^*_{L2} \\ Y_{L1} A_{L1f} V^*_{T1f} + Y_{L1} A_{L1p} V^*_{T1p} \\ Y_{L2} A_{L2f} V^*_{T2f} + Y_{L2} A_{L2p} V^*_{T2p} \\ 0 \end{bmatrix} \right] \quad (27)$$

Transforming both pressure and flow in Eq. (27) from the torn framework to the orthogonal framework using Eqs. (3), (4) and (22),

$$V_{T1f} = Y^{*-1}_{T1f} [I_{1f} - \overline{A_{T1f}} C_{T3} i_R - (\overline{A_{T1f}} Y_{T1} A_{T1p} + \overline{A_{L1f}} Y_{L1} A_{L1p}) \times V_{T1p} + \overline{A_{L1f}} Y_{L1} V_{L1}] \quad (28a)$$

$$V_{T1p} = Y^{*-1}_{T1p} [I_{1p} - \overline{A_{T1p}} C_{T3} i_R - (\overline{A_{T1p}} Y_{T1} A_{T1f} + \overline{A_{L1p}} Y_{L1} A_{L1f}) \times V_{T1f} + \overline{A_{L1p}} Y_{L1} V_{L1}] \quad (28b)$$

$$V_{T2f} = Y^{*-1}_{T2f} [I_{2f} - \overline{A_{T2f}} C_{T4} i_R - (\overline{A_{T2f}} Y_{T2} A_{T2p} + \overline{A_{L2f}} Y_{L2} A_{L2p}) \times V_{T2p} + \overline{A_{L2f}} Y_{L2} V_{L2}] \quad (28c)$$

$$V_{T2p} = Y^{*-1}_{T2p} [I_{2p} - \overline{A_{T2p}} C_{T4} i_R - (\overline{A_{T2p}} Y_{T2} A_{T2f} + \overline{A_{L2p}} Y_{L2} A_{L2f}) \times V_{T2f} + \overline{A_{L2p}} Y_{L2} V_{L2}] \quad (28d)$$

$$V_{L1} = Y^{*-1}_{L1} [i_1 - Y_{L1} A_{L1f} V_{T1f} - Y_{L1} A_{L1p} V_{T1p}] \quad (28e)$$

$$V_{L2} = Y^{*-1}_{L2} [i_2 - Y_{L2} A_{L2f} V_{T2f} - Y_{L2} A_{L2p} V_{T2p}] \quad (28f)$$

$$V_{LR} = Y^{*-1}_{LR} i_R + \overline{C_{T3}} [A_{T1f} V_{T1f} + A_{T1p} V_{T1p}] + \overline{C_{T4}} [A_{T2f} V_{T2f} + A_{T2p} V_{T2p}] \quad (28g)$$

The set of Eqs. (28a), (28b), (28c), (28d), (28e), (28f) and (28g) can now be solved to obtain the seven unknowns: V_{T1f}, V_{T2f}, I_{1p}, I_{2p}, i_1, i_2 and i_R. The solution strategy are given in the steps below:

(a) Substitute the expressions for V_{T1f} and V_{T2f} from Eqs. (28a) and (28c) into Eq. (28g) and solve the resulting equations for i_R;
(b) Back-substitute i_R into Eqs. (28a) and (28c) to get V_{T1f} and V_{T2f} respectively;
(c) Obtain the nodal flows I_{1p} and I_{2p} from Eqs. (28b) and (28d) respectively;
(d) Determine i_1 and i_2 from Eqs. (28e) and (28f) respectively.

4. Results and discussion

Two computer programs MESH and NODAL, based on mesh and nodal partitioning diakoptics respectively were written in FORTAN 77. Both programs were applied to each of the two networks SIMP and COMP (Figs. 1 and 6). Network SIMP has 9 nodes and 12 branches and is torn according to Fig. 3 for mesh diakoptics, Fig. 5 for nodal diakoptics. Network COMP has 22 nodes and 38 branches and is torn as in Fig. 7 for mesh diakoptics, Fig. 8 for nodal diakoptics. For each network the tree branches are indicated by solid lines and the links by dashed lines. The arrow in each branch represents the assumed direction of flow. All pipes in each network are assumed to be smooth with a length of 50 m and a diameter of 0.2 m. There is no active pressure source in each branch. All nodal pressures are relative to the datum which is chosen to be the highest numbered node in each case. The fluid is water with a density of 1000 kg m^{-3} and a viscosity of 0.001 kg m^{-1} s^{-1}.

For each network, analysis began with solving the problem with all nodal flows specified. These values were then verified with results obtained using the conventional partitioning approaches and used as a standard

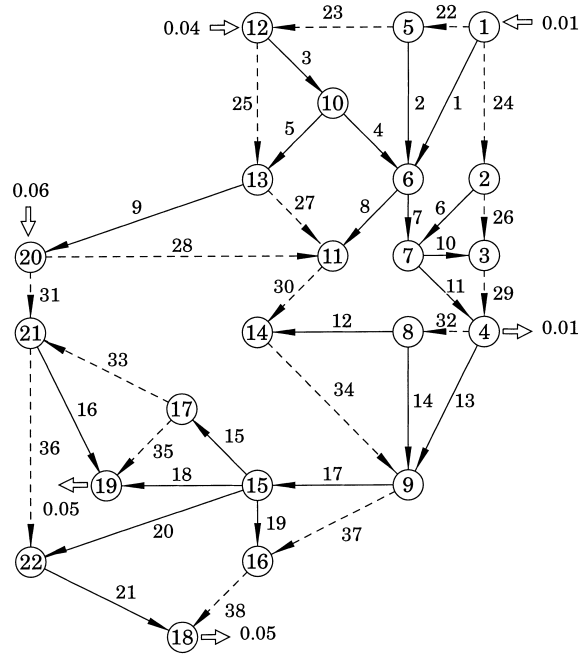

Fig. 6. Network COMP.

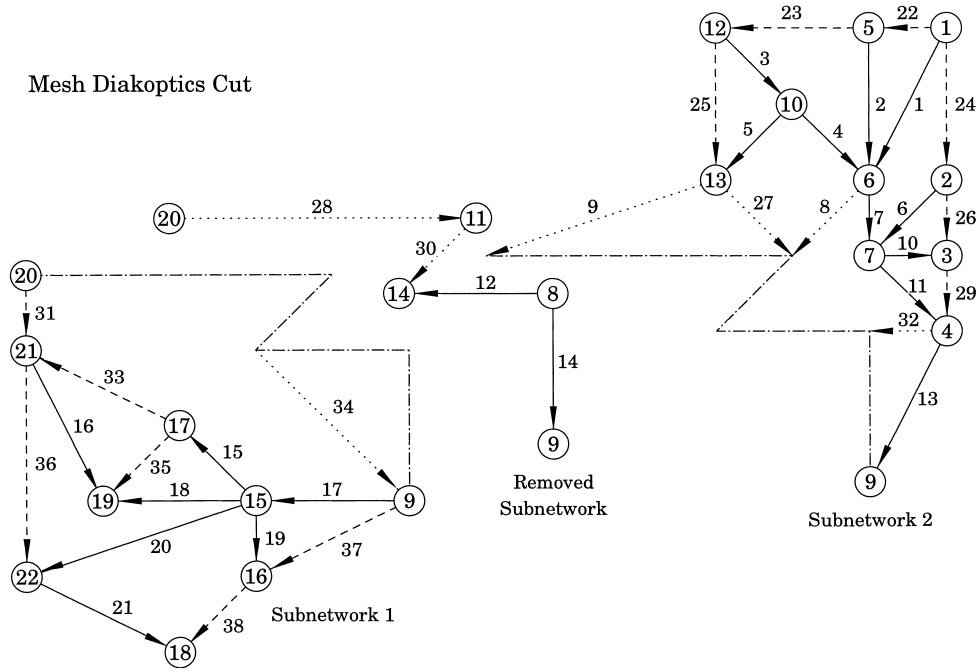

Fig. 7. Torn configuration of Network COMP cut by mesh diakoptics.

solution against which results from mixed specification simulations were compared. All simulations were run on a Pentium 133 computer with Salford FTN77/486 compiler.

Since both programs are run with a relative convergent tolerance of 0.1×10^{-5}, the results of simulations are found to be the same and are given in Tables 1 and 2 for networks SIMP and Tables 3 and 4 for networks COMP. The comparison of mixed specification to the number of iteration and computation time for each network are tabulated in Tables 5–8. Simulations were also run using a program PIPE based on mesh partitioning and results tabulated in Tables 9 and 10. Graphs of computation time per iteration against number of pressure specified nodes for networks SIMP and COMP using the various are given in Figs. 9 and 10.

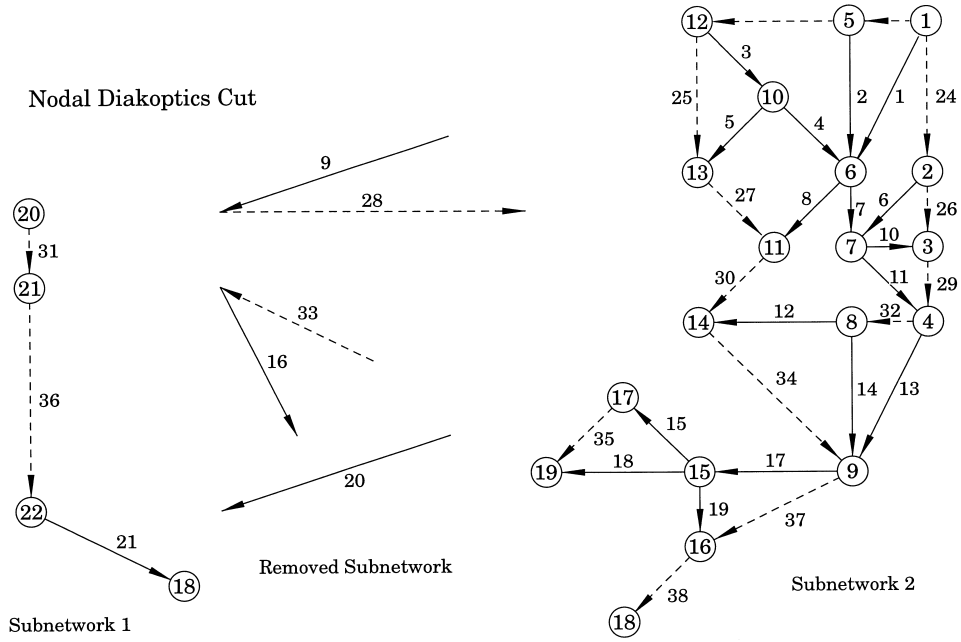

Fig. 8. Torn configuration of Network COMP cut by nodal diakoptics.

Table 1
Nodal flows and pressures for network SIMP

Node number	Flow rate ($m^3 s^{-1}$)	Pressure (Nm^{-2})
1	1.00×10^{-2}	194.43
2	0	190.50
3	2.00×10^{-2}	354.20
4	-1.50×10^{-2}	−283.48
5	0	−219.24
6	-1.50×10^{-2}	−277.95
7	0	−16.242
8	0	−9.3363

Table 2
Branch flows for network SIMP

Branch number	Flow rate ($m^3 s^{-1}$)	Branch number	Flow rate ($m^3 s^{-1}$)
1	-9.339×10^{-4}	7	1.295×10^{-3}
2	7.867×10^{-3}	8	1.541×10^{-3}
3	-1.213×10^{-2}	9	-9.066×10^{-3}
4	4.639×10^{-3}	10	-8.801×10^{-3}
5	-4.408×10^{-3}	11	-1.036×10^{-2}
6	-1.059×10^{-2}	12	-9.047×10^{-3}

Table 3
Nodal flows and pressures for network COMP

Node	Flow rate ($m^3 s^{-1}$)	Pressure (Nm^{-2})
1	1.00×10^{-2}	4043.20
2	0	3378.61
3	0	3115.12
4	-1.00×10^{-2}	2451.24
5	0	4205.96
6	0	4041.38
7	0	3246.69
8	0	2292.65
9	0	1692.30
10	0	4415.06
11	0	4027.49
12	4.00×10^{-2}	4769.71
13	0	4415.84
14	0	2483.12
15	0	209.975
16	0	212.842
17	0	175.932
18	-5.00×10^{-2}	−1190.60
19	-5.00×10^{-2}	−335.198
20	6.00×10^{-2}	4420.33
21	0	505.904

Tables 5–8 indicate that the number of iterations decreased as the number of pressure specified nodes increased. This is because, as more nodal pressures were specified, it is more likely that the nodal pressures of adjacent nodes were known. Thus more branch flows could be calculated directly from the known pressure drops. Consequently fewer iterations were required for convergence.

Table 4
Branch flows for network COMP

Branch number	Flow rate ($m^3 s^{-1}$)	Branch number	Flow rate ($m^3 s^{-1}$)
1	5.961×10^{-4}	20	9.049×10^{-3}
2	7.891×10^{-3}	21	2.386×10^{-2}
3	1.214×10^{-2}	22	-7.842×10^{-3}
4	1.250×10^{-2}	23	-1.573×10^{-2}
5	-3.607×10^{-4}	24	1.725×10^{-2}
6	6.966×10^{-3}	25	1.213×10^{-2}
7	1.905×10^{-2}	26	1.028×10^{-2}
8	1.937×10^{-3}	27	1.277×10^{-2}
9	-1.009×10^{-3}	28	1.286×10^{-2}
10	6.956×10^{-3}	29	1.724×10^{-2}
11	1.906×10^{-2}	30	2.757×10^{-2}
12	-8.567×10^{-3}	31	4.613×10^{-2}
13	1.857×10^{-2}	32	7.728×10^{-3}
14	1.629×10^{-2}	33	-1.166×10^{-2}
15	3.234×10^{-3}	34	1.900×10^{-2}
16	1.966×10^{-2}	35	1.489×10^{-2}
17	2.695×10^{-2}	36	1.481×10^{-2}
18	1.544×10^{-2}	37	2.692×10^{-2}
19	-7.768×10^{-4}	38	2.614×10^{-2}

Table 5
Mixed specification simulations for network SIMP (mesh partitioning diakoptics)

No. of pressure specified nodes	No. of iterations	Computation time (s)	Computation time per iteration (s)
0	22	0.05469	0.002486
1	22	0.05469	0.002486
2	22	0.05469	0.002486
3	21	0.05469	0.002604
4	21	0.05469	0.002604
5	20	0.05469	0.002735
6	21	0.05469	0.002604
7	19	0.05469	0.002878
8	2	–	–

Table 6
Mixed specification simulations for network SIMP (nodal partitioning diakoptics)

No. of pressure specified nodes	No. of iterations	Computation time (s)	Computation time per iteration (s)
0	22	0.05469	0.002486
1	22	0.05469	0.002486
2	22	0.05469	0.002486
3	21	0.05469	0.002604
4	20	0.05469	0.002735
5	20	0.05469	0.002735
6	19	0.05469	0.002878
7	19	0.05469	0.002878
8	2	–	–

The least number of iterations is found in the case where all the nodal pressures were specified, in which all the branch flows could be computed immediately and convergence was attained in just two iterations.

Table 7
Mixed specification simulations for network COMP (mesh partitioning diakoptics)

No. of pressure specified nodes	No. of iterations	Computation time (s)	Computation time per iteration (s)
0	24	0.27344	0.01139
1	24	0.49609	0.02067
2	24	0.54688	0.02279
3	23	0.49609	0.02157
4	24	0.49219	0.02051
5	23	0.49219	0.02140
6	24	0.49609	0.02067
7	23	0.49609	0.02157
8	23	0.49219	0.02140
9	22	0.49219	0.02237
10	22	0.49219	0.02237
11	22	0.49609	0.02255
12	21	0.49609	0.02362
13	21	0.49219	0.02344
14	21	0.49219	0.02344
15	21	0.49219	0.02344
16	21	0.49609	0.02362
17	21	0.49609	0.02362
18	21	0.44141	0.02102
19	21	0.49619	0.02344
20	20	0.44141	0.02207
21	2	0.10938	0.05469

The first row of results in Tables 7, 8 and 10 shows the number of iteration and computation time for fully flow-specified problem using mesh partitioning diakoptics, nodal partitioning diakoptics and mesh partitioning respectively,

Table 8
Mixed specification simulations for network COMP (nodal partitioning diakoptics)

No. of pressure specified nodes	No. of iterations	Computation time (s)	Computation time per iteration (s)
0	24	0.93359	0.03890
1	24	0.93359	0.03890
2	24	0.87891	0.03662
3	24	0.82422	0.03434
4	24	0.82422	0.03434
5	22	0.71484	0.03249
6	22	0.71484	0.03249
7	22	0.71484	0.03249
8	22	0.71484	0.03249
9	22	0.71484	0.03249
10	22	0.71484	0.03249
11	22	0.65625	0.02983
12	22	0.66016	0.03000
13	21	0.65625	0.03125
14	21	0.71484	0.03404
15	21	0.71484	0.03404
16	21	0.76953	0.03664
17	21	0.76953	0.03664
18	19	0.71484	0.03762
19	19	0.76953	0.04050
20	18	0.71484	0.03971
21	2	0.16406	0.08203

Table 9
Mixed specification simulations for network SIMP using program PIPE (mesh partitioning)

No. of pressure specified nodes	No. of iterations	Computation time (s)	Computation time per iteration (s)
0	22	0.10938	0.00497
1	22	0.10938	0.00497
2	22	0.16406	0.00746
3	21	0.10938	0.00521
4	21	0.10938	0.00521
5	20	0.10938	0.00547
6	21	0.10938	0.00521
7	19	0.10938	0.00576
8	2	0.05469	0.02735

applied to the large network COMP. The number of iterations were the same for each method (24 iterations) but in terms of computation time per iteration, both mesh and nodal partitioning diakoptics were much faster than mesh partitioning. Computation time per iteration for mesh partitioning diakoptics was less than 12% and nodal partitioning diakoptics about 40% of that for mesh partitioning. Results for mixed specification also indicate that partitioning diakoptics is more superior in efficiency than the conventional partitioning methods (See Figs. 9 and 10).

The most time-consuming process in computation is matrix inversion. The larger the matrix the longer is the time required for inversion. Since diakoptics tears a given network into smaller units, the matrices that result have a smaller dimension than those in the untorn network.

Table 10
Mixed specification simulations for network COMP using program PIPE (mesh partitioning)

No. of pressure specified nodes	No. of iterations	Computation time (s)	Computation time per iteration (s)
0	24	2.30469	0.09603
1	24	2.36328	0.09847
2	24	2.30859	0.09619
3	23	2.25391	0.09800
4	24	2.36328	0.09847
5	23	2.25000	0.09783
6	24	2.36328	0.09470
7	23	2.36328	0.10275
8	23	2.36328	0.10275
9	22	2.25000	0.10227
10	22	2.30469	0.10476
11	22	2.30469	0.10476
12	21	2.25391	0.10733
13	21	2.30469	0.10975
14	21	2.30859	0.10993
15	21	2.41797	0.11514
16	21	2.47266	0.11775
17	21	2.52734	0.12035
18	21	2.58203	0.12295
19	21	2.69141	0.12816
20	20	2.64063	0.13053
21	2	0.38672	0.19336

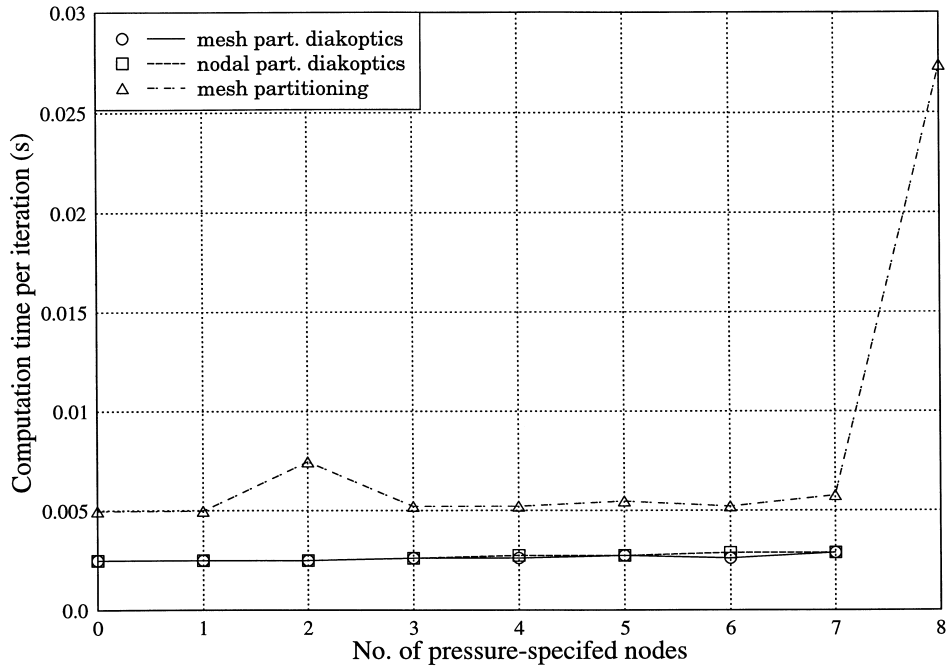

Fig. 9. Graph of computation time per iteration against number of pressure specified nodes for network SIMP.

Accordingly their inversion is faster than those in the untorn network.

Between mesh and nodal partitioning diakoptics the former seems more efficient than the latter. A closer examination of the way network COMP is torn reveals that subnetwork 2 in the torn configuration for nodal diakoptics, having 30 branches and 18 nodes, is considerably larger than the subnetworks in the torn configuration for mesh diakoptics. Consequently the matrices to be inverted are larger than those involved in mesh diakoptics. Since there is usually more than one way of tearing a given network, nodal partitioning diakoptics can be more efficient if network

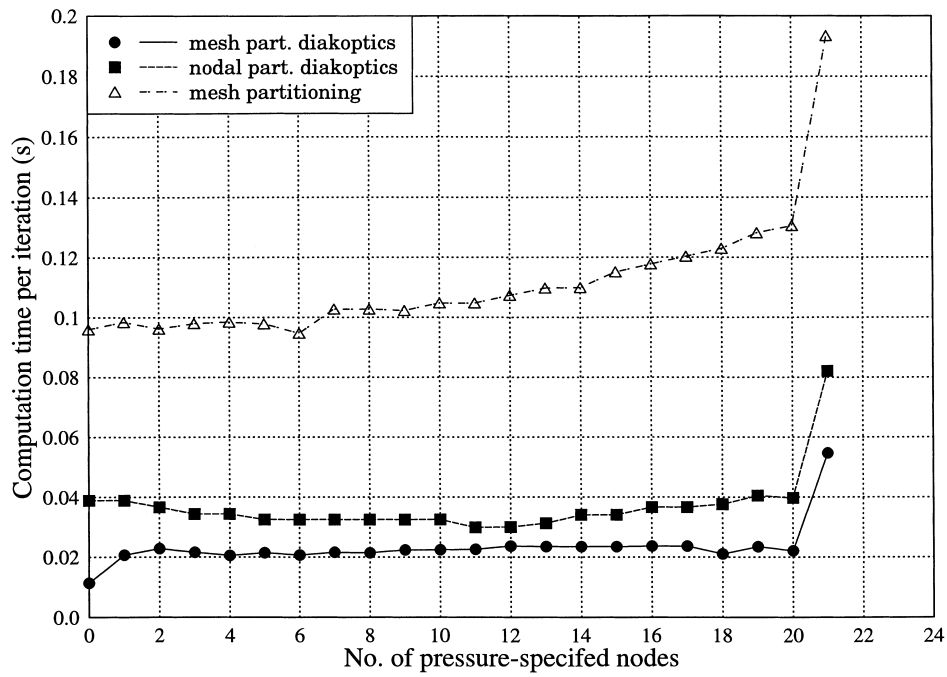

Fig. 10. Graph of computation time per iteration against number of pressure specified nodes for network COMP.

Table 11
Mixed specification simulations for network COMP (nodal partitioning diakoptics on new torn configuration as in Fig. 11)

No. of pressure specutationified nodes	No. of iterations	Computation time (s)	Computation time per iteration (s)
0	24	0.43750	0.01823
1	24	0.44141	0.01839
2	24	0.44141	0.01839
3	24	0.44141	0.01839
4	24	0.38672	0.01611
5	24	0.44141	0.01839
6	24	0.38672	0.01611
7	24	0.38281	0.01595
8	24	0.38281	0.01595
9	24	0.38672	0.01611
10	23	0.38281	0.01664
11	22	0.38672	0.01758
12	23	0.38672	0.01681
13	22	0.33203	0.01509
14	22	0.32813	0.01491
15	22	0.38281	0.01740
16	22	0.38281	0.01740
17	21	0.32813	0.01563
18	21	0.38672	0.01842
19	19	0.38672	0.02035
20	19	0.38281	0.02015
21	2	0.05469	0.02934

COMP is torn into subnetworks that are comparable in size, so that the matrices to be inverted would have a smaller dimension. Table 11 gives the results of mixed specification simulations using nodal partitioning diakoptics applied to network COMP, but with the network being torn as in Fig. 11 into two subnetworks of comparable size. Fig. 12 is a plot of computation time per iteration against number of pressure-specified nodes using mesh partitioning diakoptics applied to the original torn configuration as in Fig. 7, nodal partitioning diakoptics applied to the original torn configuration as in Fig. 8 and partitioning diakoptics applied to the new torn configuration as in Fig. 11. These results show that nodal partitioning diakoptics applied to the new torn configuration gives the fastest computation time. Therefore, whether mesh or nodal partitioning diakoptics is more efficient depends on how the network is torn for each method. Comparing the convergence time required for diakoptics in the present work with that in the literature [8], it appears that the computation time is much shorter in the present work. However, convergence time in this instance does not form a valid basis for comparison. This is because in the program in Ref. [8] direct access file was used to store information pertaining to each subnetwork. At any time, only the required subnetwork's information was read. Thus the program involved a lot of input/output, which took up a lot of time. With improved technology, however, storage does not pose a great problem nowadays. Therefore, the use of the direct access file is discarded in the present study.

5. Conclusion

Partitioning diakoptics has been found to be more efficient than conventional partitioning methods in solving mixed specifications problems in fluid pipe networks, by reducing computation time significantly especially when the given network is very large. This is due to tearing of the parent network into smaller subnetworks in the diakoptics approach, resulting in matrices of smaller dimension which can be more easily inverted. Whether mesh or nodal parti-

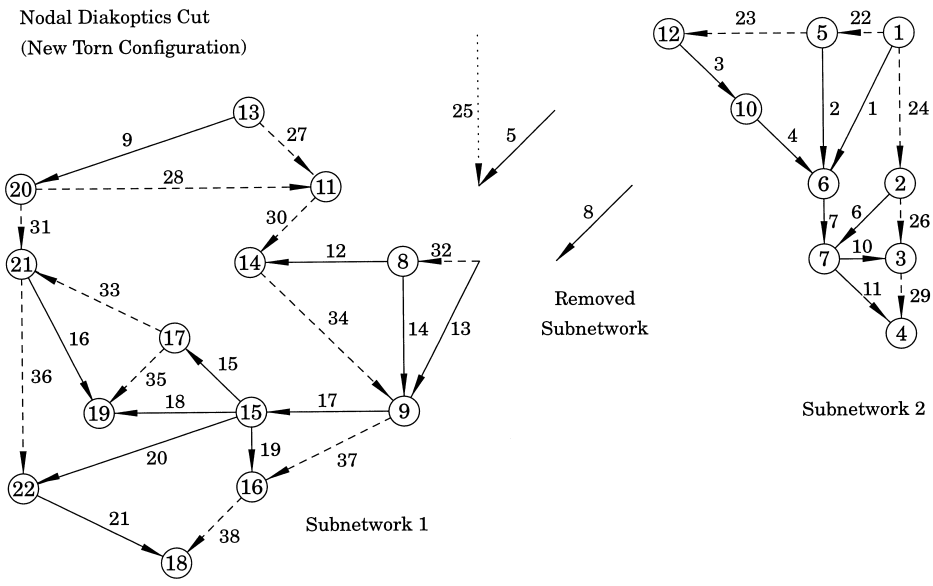

Fig. 11. New torn configuration of Network COMP cut by nodal diakoptics.

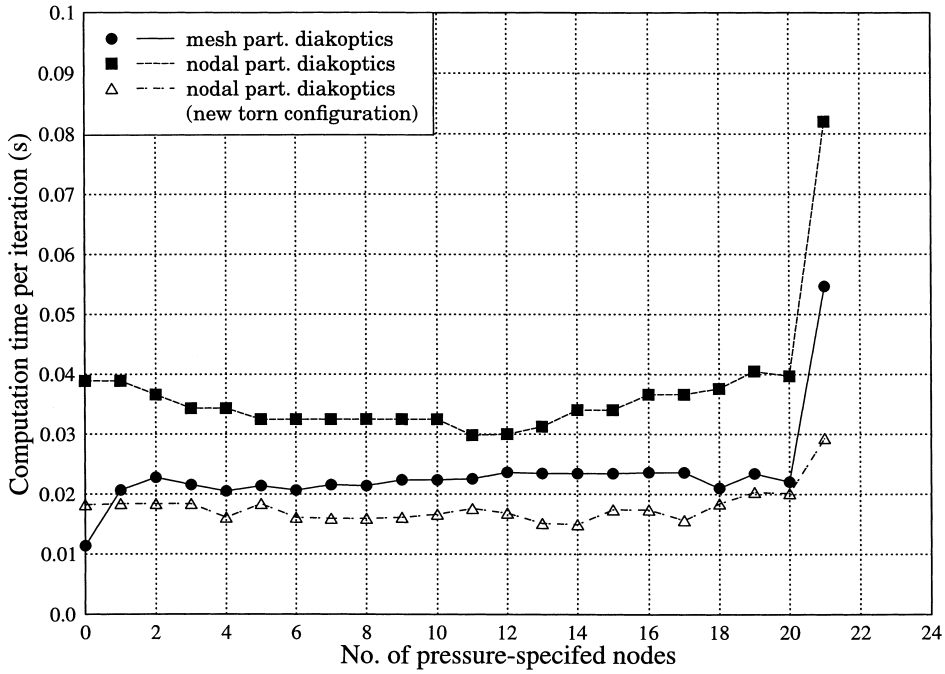

Fig. 12. Graph of computation time per iteration against number of pressure specified nodes for network COMP.

tioning diakoptics is more efficient depends on how the network is torn for each method.

6. List of Notation

A	Branch-node incidence matrix of a network; Transformation tensor used in nodal partitioning diakoptics
B	Node-to-datum path matrix.
C	Branch-mesh incidence matrix of a network; Transformation tensor used in mesh partitioning diakoptics
D	Diameter of a pipe
I	Contravariant tensor for flow due to external input–output on a branch of path; Nodal flow
i	Contravariant tensor for flow due to other causes on a branch or path; Mesh flow
J	Contravariant tensor for total flow on a branch or path, in primitive framework, $J=I+i$
L	Length of pipe
ΔP	Pressure drop across a pipe, which is equivalent to V in the matrix analysis
Q	Volumetric flow rate through a pipe, which is equivalent to J in the matrix analysis
U	Identity matrix
V	Covariant tensor for total pressure, in primitive framework
Y	Contravariant tensor for admittance, used in the nodal approach
Z	Covariant tensor for impedance, used in the mesh approach

6.1. Greek symbols

π	Ratio of circumference to diameter of a circle
ρ	Density of fluid
ϕ_f	Fanning friction factor

6.2. Index nomenclature

b	Index used in tensor form, indicating the tensor to be in primitive framework
c	Index used in tensor form, indicating the tensor to be in closed path framework
L	Index used for matrix form, indicating that the matrix involves the link branches
o	Index used in tensor form, indicating the tensor to be in open framework
p	Index used in tensor form, indicating the tensor to be in torn framework
R	Index used in matrix form, indicating that the matrix pertains to the removed subnetwork
s	Index used in tensor form, indicating the tensor to be in orthogonal framework
T	Index used in matrix form, indicating that the matrix involves the tree branches
1	Index used in matrix form, indicating that the matrix pertains to subnetwork 1 only
2	Index used in matrix form, indicating that the matrix pertains to subnetwork 2 only
3	Index used in matrix form, indicating that the matrix pertains to subnetwork 1 and the removed subnetwork

4	Index used in matrix form, indicating that the matrix pertains to subnetwork 2 and the removed subnetwork
1f	Index used in matrix form, indicating that the matrix pertains to subnetwork 1 and the in the flow-specified framework
1p	Index used in matrix form, indicating that the matrix pertains to subnetwork 1 and in the pressure-specified framework
2f	Index used in matrix form, indicating that the matrix pertains to subnetwork 2 and in the flow-specified framework
2p	Index used in matrix form, indicating that the matrix pertains to subnetwork 2 and in the pressure-specified framework
Rf	Index used in matrix form, indicating that the matrix pertains to the removed subnetwork 1 and in the flow-specified framework
Rp	Index used in matrix form, indicating that the matrix pertains to the removed subnetwork and in the pressure-specified framework
*	Index used in matrix form, indicating that the matrix pertains to the torn framework

6.3. Matrix notation

$\bar{M}$	Transpose of matrix **M**
M^{-1}	Inverse of matrix **M**

References

[1] G. Kron, Tensor Analysis of Networks, 2nd ed., Macdonald, London, 1965.
[2] B. Gay, P. Middleton, The solution of pipe network problems, Chem. Eng. Sci. 26 (1971) 109–123.
[3] B. Gay, P.E. Preece, Matrix methods for the solution of fluid network problems: mesh methods, Trans. Instn. Chem. Eng. 53 (1975) 12–15.
[4] H.C. Ti, E.T. Kang, Tensor Analysis of Fluid Network Problems, Proceedings of Fourth Asian Pacific Confederation of Chemical Engineering, (APCChE'87), Singapore, 1987, pp. 569–575.
[5] H.C. Ti, Mixed specification problems in pipeline network analysis: partitioning methods, Chem. Eng. J. 44 (1990) 89–95.
[6] H.H. Happ, Diakoptics and Networks, Academic Press, New York, 1971.
[7] B. Gay, P.E. Preece, Matrix methods for the solution of fluid network problems: diakoptics methods, Trans. Instn. Chem. Eng. 55 (1977) 38–45.
[8] H.C. Ti, P.E. Preece, Large-scale fluid network analysis: mixed pressure and flow specification, Chem. Eng. J. 50 (1992) 133–141.